

## Electrochemical studies on emulsion coated mild steel in ground water

V.I. Jasmine,<sup>1</sup> P.S.L.M. Kala,<sup>1</sup> M.J. Clara,<sup>1</sup> H.M. Banu,<sup>1</sup> A. Nirmala,<sup>1</sup>  
N. Anitha,<sup>1</sup> A. Krishnaveni<sup>2</sup> and S. Rajendran<sup>1,3</sup> \*

<sup>1</sup>Corrosion Research Centre, Department of Chemistry, St Antony's College of Arts and Sciences for Women, Dindigul, 624005, Tamil Nadu, India (Affiliated to Mother Teresa Women's University, Kodaikanal, Tamil Nadu, India)

<sup>2</sup>PG Department of Chemistry, Yadava College, Natham Road, Tiruppalai, Madurai, Tamil Nadu 625007, India

<sup>3</sup>Adjunct Professor, Centre for Nanoscience and Technology, Pondicherry University, Chinna Kalapet, Kalapet, Puducherry 605014, India

\*E-mail: [susairajendran@gmail.com](mailto:susairajendran@gmail.com)

### Abstract

The corrosion resistance of mild steel immersed in groundwater before and after Emulsion coating has been evaluated by electrochemical studies such as polarization study and AC impedance spectroscopy. When a protective film (emulsion coating) is formed on metal surface, corrosion resistance of the metal increases and hence LPR value increases and corrosion current decreases. Similarly, when a protective film is formed on the metal surface, corrosion resistance increases,  $R_t$  values, impedance values and phase angle increase whereas  $C_{dl}$  values decrease. Electrochemical studies reveal that the corrosion inhibition efficiency of mild steel after emulsion coating is found to be greater than 95%. Electrochemical studies lead to the conclusion that the mild steel tank used in water storing may be given a coat of emulsion coating to improve the life time of the mild steel tank. Mild steel pipelines carrying ground water may be given an inner emulsion coating. AFM study reveals that the film coating is at nano scale level. The AFM parameters, namely, RMS ( $S_q$ ) roughness (nm), average ( $S_a$ ) roughness (nm), and maximum peak-to-valley height ( $S_y$ ) (nm) for the coated system are lower than those for uncoated system. That is after coating, the surface of mild steel becomes smoother. Analysis of SEM images confirms that the coated surface is smoother than the uncoated surface. Contact angle measurement study reveals that after emulsion coating, the mild steel surface becomes hydrophobic in nature. It acquires water repelling nature. So, corrosion inhibition efficiency is greater than 95%. The findings will be useful in transport of mild steel pipelines carrying ground water.

Received: January 25, 2024. Published: March 7, 2024

doi: [10.17675/2305-6894-2024-13-1-27](https://doi.org/10.17675/2305-6894-2024-13-1-27)

**Keywords:** electrochemical studies, emulsion coating, mild steel, ground water, AMF, SEM, contact angle measurement, hydrophobicity.

## Introduction

The detrimental impact of corrosion on metallic materials remains a pressing concern across industries. Recently, intelligent anti-corrosive coatings for safeguarding metal infrastructures have gained significant interest. These coatings are equipped with micro/nano carriers that store corrosion inhibitors and release them when triggered by external stimuli. These advanced coatings have the capability to elevate the electrochemical impedance values of steel by 2–3 orders of magnitude compared to the blank coating. However, achieving intelligent, durable, and reliable anti-corrosive coatings requires careful consideration in the design of these micro/nano carriers. Many research works have been carried out in the field of corrosion inhibition by various types of coatings [1–10].

Nano zero-valent iron (NZVI) is an ideal material for treating chromium (VI). However, the NZVI's low loading and corrosion susceptibility in acidic Cr-containing industrial wastewater is the most pressing issue. Therefore, it is necessary to explore a method to construct novel NZVI composites with high loading, corrosion resistance, and outstanding activity. A green 2-mercaptobenzimidazole (MBI) was employed by Yang *et al.* [1], for the first time as a corrosion inhibitor for NZVI to form a protective coating through chemisorption, thus blocking the corrosion of NZVI by reaction medium.

Two-dimensional materials have been proved to be effective in improving the performance of anticorrosive coatings. However, most of the reported two-dimensional materials only have the ability to passively block corrosive media and cannot effectively inhibit localized corrosion reactions at the metal/coating interface. Hu *et al.* [2] have synthesized a novel polyaniline (PANI) nanosheet with both barrier and passivation functions for metals. In addition, polydopamine (PDA) wrapped PANI nanosheets (PANI@PDA) were obtained by in situ self-polymerization reaction of dopamine on the PANI surface, which enhance its interfacial interaction with polymeric resin. The chemical structure, morphology and corrosion inhibition properties of the nanosheets were systematically analyzed [2].

Nanocomposite coatings based on polydimethylsiloxane were developed by Ghamari *et al.* [3] by adding silver phosphate and titania nanoparticles with a PDMS pre-layer for 316L stainless steel. FTIR spectra and XRD patterns confirmed the synthesis of  $\text{TiO}_2$  and  $\text{Ag}_3\text{PO}_4$  nanoparticles and nanocomposite coating. FESM and AFM images show that with the increase of  $\text{Ag}_3\text{PO}_4$  nanoparticles, the roughness of coatings increased [3].

Although Polyindole (Pind) with a  $\pi$ -conjugated polymeric structure has been regarded as a promising organic material, the loosely packed and brittle backbones still hinder its long-term usage stability for various applications. Herein, a novel Pind/MXene composite with a 3D robust architecture has been developed by Chen *et al.* [4] by confining Pind nanoparticles in layered MXene through a simple and mild polymerization approach, which shows unique dual functionality for energy storage and corrosion protection for the first time.

The tribocorrosion performance of hydrogenated and hydrogen-free diamond-like carbon (DLC) coated thermal sprayed WC-based cermet/carbide were investigated

comparatively by Zhang *et al.* [5]. The results showed that, regardless of hydrogen containing, both coatings demonstrated the improvement of anti-tribocorrosion capability of WC-based cermet in 3.5 wt.% NaCl solution, by suppressing the corrosion of Ni-based binder phases.

A strategy based on *in situ* host-guest nanoconfinement was used by Wei *et al.* [6] to assist the synthesis of a ZIF-8 host loaded with a corrosion inhibitor 8-hydroxyquinoline (8-HQ) guest by a facile one-step process at room temperature. Results showed that a Zn-(bis-8-hydroxyquinoline) guest encapsulated ZIF-8 host composite (Q@ZIF-8) was formed. The Q@ZIF-8 proves to have an inhibition efficiency of over 91% to protect the aluminum alloy substrate against corrosion in the corrosive solution after 2 days. Additionally, the pH-responsive Q@ZIF-8 can release 8-HQ species in form of hydroxyquinoline zinc complex and improves the corrosion resistance of the epoxy coating [6].

It is of great convenience and economy to incorporate novel functionalized nanofillers with superior anticorrosive properties to further elevate the corrosion protective period of epoxy coating. For this purpose, Xia *et al.* [7] fabricated finely dispersed cerium oxide grafting polydopamine modified graphitic carbon nitride ( $g\text{-C}_3\text{N}_4\text{@PDA@CeO}_2$ ) via self-polymerization method and hydrothermal technique to promote the epoxy coating's anticorrosion performance on P110 substrate. The XRD, XPS, TGA, and SEM analyses were employed to qualitatively verify the successful synthesis of  $g\text{-C}_3\text{N}_4\text{@PDA@CeO}_2$  nanocomposite [7].

Biofouling, the accumulation of microorganisms, plants, algae on wet surfaces is one of the major issues adversely affecting the overall hydrodynamic performance of the marine vessels. Ceria ( $\text{CeO}_2$ ) nanoparticles (NPs) are effectively used as anti-biofouling agent to prevent the deterioration of steel structures, due to their excellent redox capacity. Various approaches are being investigated to enhance the antifouling activity of ceria NPs. Vijayan *et al.* [8] have reported the development of novel polydopamine (PDA) functionalised ceria-zirconia nanoparticles filled water-borne epoxy nanocomposite coating to prevent the microbial-induced corrosion of mild steel. Ceria NPs were functionalised with PDA to enhance the dispersibility and improve their ability to resist biofouling in water-borne epoxy resin coatings against microbial species [8].

Hydrogen embrittlement in hydrogen pipelines can cause severe economic losses and safety hazards, thus research on efficient hydrogen barrier coatings is of great importance. In this study, a more efficient and easily operable non-covalent modification method was employed to modify carboxymethyl chitosan (CMCS) onto graphene oxide (GO), resulting in a significant improvement in the dispersibility and uniform distribution of GO in waterborne epoxy resin. Subsequently, a hydrogen barrier coating was prepared by Wan *et al.* [9] by incorporating the modified GO into waterborne epoxy resin. The influence of different doping concentrations on the coating performance was investigated. The basic properties of the coatings were characterized using macroscopic analysis, SEM, contact angle measurements, adhesion tests and electrochemical techniques. The corrosion

resistance and hydrogen barrier effect were evaluated through electrochemical hydrogen permeation experiments. Results showed that the modified graphene oxide has good compatibility with epoxy resin [9].

Two-dimensional transition metal carbides and carbon nitride (MXene) and mesoporous silica nanoparticles ( $\text{SiO}_2$ ) loaded with corrosion inhibitor 1-(3-((*N-n*-butyl) aminocarboxamido)propyl)-3-hexadecyl imidazolidin bromide (M16) were used by Li *et al.* [10] to prepare a M16@MXene- $\text{SiO}_2$  nanocomposite with good anti-corrosion and wear resistance. The structure and composition of the nanocomposites were characterized by scanning electron microscopy (SEM), transmission electron microscopy (TEM), Fourier transform infrared (FT-IR), thermogravimetric analysis (TGA) and X-ray photoelectron spectroscopy (XPS). The synthesized M16@MXene- $\text{SiO}_2$  nanocomposite was then added to an epoxy coating on Q235 carbon steel. The uniform distribution of M16@MXene- $\text{SiO}_2$  in the coating was confirmed by SEM and atomic force microscopy (AFM) [10].

The present work is undertaken to investigate the corrosion resistance of mild steel in ground water before after an emulsion coating. Electrochemical studies such as polarization study and AC impedance spectra have been employed for this purpose. The surface morphology has been characterized by techniques such as SEM, AFM and contact angle measurement. The outcome of the study will be used to store ground water in mild steel water tanks coated with the proposed emulsion coating. Further mild steel pipelines carrying ground water may be given an inner coating of this proposed emulsion namely, Nippon paint Weatherbond PRO exterior emulsion coating (pink) [emulsion coating].

## Experimental

### *Mild steel*

The mild steel electrodes were polished to mirror finish with different grade emery sheets, degreased with trichloroethylene. The emulsion coating was done by spray coating method.

### *Electrochemical studies*

Electrochemical studies such as polarization study and AC impedance spectra have been widely used in corrosion inhibition study [11–20].

### *Polarization study*

In the present work, corrosion resistance of mild steel immersed in ground water was measured by potentiodynamic polarization study. The experiments were done at room temperature. Polarization studies were carried out in a CHI- electrochemical work station with impedance model 660A. It was provided with iR compensation facility. A three-electrode cell assembly was used. Mild steel was used as working electrode, platinum as counter electrode and saturated calomel electrode (SCE) as reference electrode. From polarization study, corrosion parameters such as corrosion potential ( $E_{\text{corr}}$ ), corrosion current

density ( $i_{\text{corr}}$ ), Tafel slopes anodic  $b_a$  and cathodic  $b_c$ , and linear polarization resistance (LPR) value were calculated.

### *AC Impedance spectra*

AC impedance spectra have been used to investigate the formation of a protective film during corrosion protection process.

In the present study, the same instrument and cell set-up used for polarization study was used to record AC impedance spectra also. A time interval of 5 to 10 minutes was given for the system to attain a steady state open circuit potential. The real part ( $Z'$ ) and imaginary part ( $-Z''$ ) of the cell impedance were measured in ohms at various frequencies.

Charge transfer resistance ( $R_t$ ) and double layer capacitance ( $C_{\text{dl}}$ ) were calculated:

$$R_t = (R_s + R_t) - R_s$$

where  $R_s$  = solution resistance.  $C_{\text{dl}}$  values were calculated using the relationship

$$C_{\text{dl}} = 1/2\pi f_{\text{max}} \cdot R_t$$

where  $f_{\text{max}}$  = frequency at maximum imaginary impedance.

### *Surface characterization study*

The mild steel specimens were immersed in ground water for a period of one day. After one day the specimens were taken out and dried. The nature of the film formed on the metal surface was analyzed by surface characterization studies such as scanning electron microscopy (SEM) and atomic force microscopy (AFM) and contact angle measurement.

### *Scanning electron microscopy (SEM)*

The mild steel specimens immersed in various test solutions for one day were taken out, dried and subjected to the surface examination. The surface morphology measurements of the mild steel surface were carried out by scanning electron microscopy (SEM) using CAREL ZEISS make model EVO-18.

### *Atomic force microscopy (AFM)*

The mild steel specimens immersed in various test solutions for one day were taken out, dried and subjected to the surface examination. The surface morphology measurements of the mild steel surface were carried out by atomic force microscopy (AFM) using SPM Veeco Dinnova connected with the software version V7.00 and the scan rate of 0.7 Hz.

### *Contact angle measurements*

The contact angle is the angle quantifying the wettability of a solid surface by a liquid. The adsorption nature of the inhibitor on the surface of the mild steel was verified by determining the contact angle. The contact angle measurement on the surface were performed on a VCA

---

optima instrument equipped with CCD camera for imaging. The deionized water under static conditions with a drop volume of 5  $\mu\text{L}$  was employed to determine the contact angle. VCA optima XC software provided with instruments was used for fitting the drop shapes to find the contact angle of water on the surface.

## Results and Discussion

Paint is any pigmented liquid, liquefiable, or solid mastic composition that, after application to a substrate in a thin layer, converts to a solid film. It is most commonly used to protect, color, or provide texture. It has been used in the corrosion inhibition study as well.

The present work is undertaken to investigate the corrosion resistance of mild steel immersed in groundwater before and after coating of Nippon paint Weatherbond PRO exterior emulsion coating (pink) [emulsion coating]. The corrosion resistance has been evaluated by electrochemical studies such as polarization study and AC impedance spectra [11–20].

### *Analysis of results of electrochemical studies*

Corrosion resistance of mild steel immersed in groundwater, before and after Weatherbond PRO emulsion coating (Emulsion coating) has been evaluated by polarization study and AC impedance spectroscopy [11–20].

### *Analysis of results of polarization study*

The polarization curves of mild steel immersed in groundwater before and after weather bond pro emulsion coating (Emulsion coating) are shown in Figure 1. Potential vs current plots of mild steel, before coating (a) and after coating (b) immersed in ground water are shown in Figure 2.

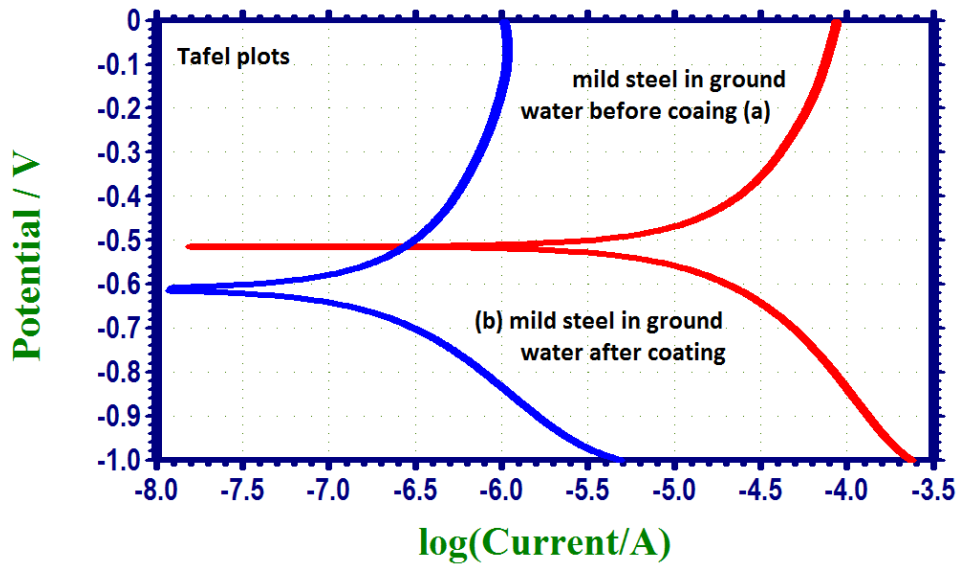


**Figure 1.** Tafel plots of mild steel, before coating (a) and after coating (b) immersed in ground water.

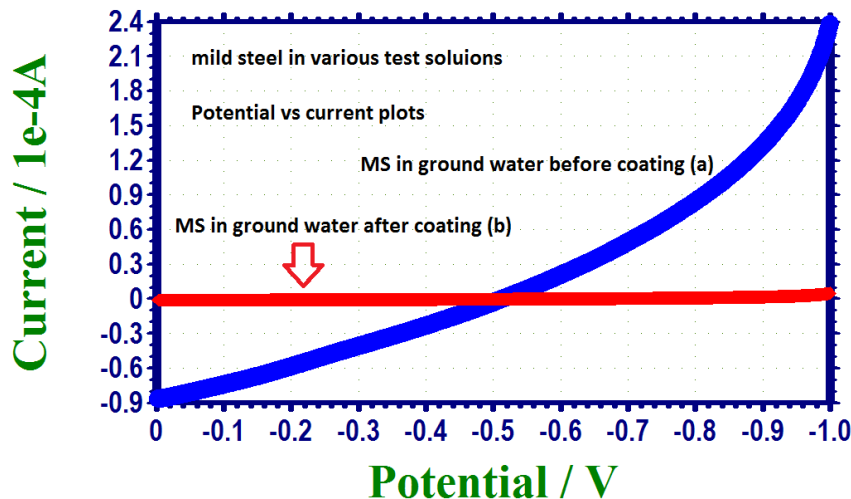


**Figure 2.** Potential vs current plots of mild steel, before coating (a) and after coating (b) immersed in ground water.

The corrosion parameters, namely, corrosion potential ( $E_{\text{corr}}$ ), Tafel slopes ( $b_c$ =cathodic;  $b_a$ =anodic), linear polarization resistance (LPR) and corrosion current density ( $i_{\text{corr}}$ ) are given in Table 1.

#### *Potential vs. current plots*

When mild steel is immersed in ground water, the variation in potential (from  $-0.1$  to  $-1.0$  V) resulted in an augment in current. Interestingly after emulsion coating when potential was varied there was no change in the current passing through the electrode

(Figure 2). This means that the emulsion coating present on the mild steel is very stable. It is not broken by the ions present in the ground water under investigation.

**Table 1.** Corrosion parameters of mild steel before coating and after coating immersed in various test solution obtained by polarization study.

System	$E_{\text{corr}}$ vs. SCE mV	$b_c$ mV/decade	$b_a$ mV/decade	LPR Ohm·cm <sup>2</sup>	$i_{\text{corr}}$ A/cm <sup>2</sup>
Mild steel in ground water	−515	191	219	$4.41 \cdot 10^3$	$101 \cdot 10^{-7}$
MS after coating in ground water	−612	186	226	$3.16 \cdot 10^5$	$1.40 \cdot 10^{-7}$
Inference	Cathodic shift. Cathodic reaction controlled predominantly			LPR increases. Corrosion resistance increases	$i_{\text{corr}}$ decreases. Corrosion resistance increases
Implication	After emulsion coating, corrosion resistance of mild steel in ground water increases. Mild steel tanks used to store ground water may be given an emulsion coating. Mild steel pipelines carrying ground water may be given an inner emulsion coating.				

According to the principles of polarization study, when a protective film (emulsion coating) is formed on metal surface, corrosion resistance of the metal increases and hence LPR value increases and corrosion current decreases (Figures 1–3).

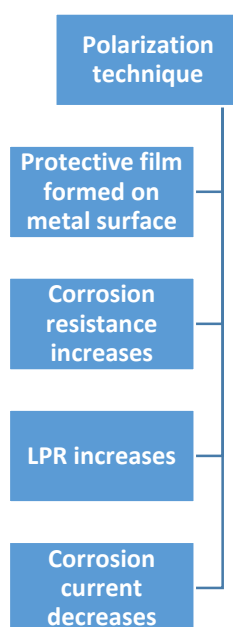


**Figure 3.** Correlation among corrosion parameters of polarization study.

It is observed from Table 1 and Figure 1 that after emulsion coating, the corrosion resistance of mild steel in groundwater increases because the LPR value increases and corrosion current decreases. Corrosion inhibition efficiency of 98.61% (calculated from LPR values) is offered by the emulsion coating. Inhibition efficiency was calculated using the relation

$IE = [(LPR1 - LPR2) / LPR1] \cdot 100\%$ , where LPR1 is the linear polarization resistance value in the presence of coating and LPR2 is the linear polarization resistance value in the absence of coating.

#### *Analysis of results of AC impedance spectroscopy*

The AC impedance spectra of mild steel immersed in groundwater in the absence and presence of emulsion coating are shown in Figures 4–14. The Nyquist plots are shown in Figures 4 and 8. The Bode plots are shown in Figures 5 and 9. The interactive 3D plots are shown in Figures 6, 7, 10 and 11. The equivalent circuit diagram for Figures 4 and 8 is shown in Figure 15.

The corrosion parameters such as charge transfer resistance ( $R_t$ ), impedance value, phase angle values and double layer capacitance ( $C_{dl}$ ) values are given in Table 2.

**Table 2.** Corrosion parameters of mild steel immersed in groundwater before and after pink emulsion coating (emulsion coating) obtained by AC impedance spectra.

System	$R_t$ Ohm·cm <sup>2</sup>	Impedance log(Z/Ohm)	$C_{dl}$ F/cm <sup>2</sup>	Phase angle degrees
Mild steel in ground water	$8.99 \cdot 10^2$	3.038	$56.75 \cdot 10^{-10}$	40.39
Mild steel coated with Pink Emulsion in ground water	$4.77 \cdot 10^4$	4.683	$1.07 \cdot 10^{-10}$	81.89
Inference	Increases. Corrosion resistance increases	Increases. Corrosion resistance increases	Decreases. Corrosion resistance increases	Increases. Corrosion resistance increases
Implication	After emulsion coating, corrosion resistance of mild steel in ground water increases. Mild steel tanks used to store ground water may be given an emulsion coating. Mild steel pipelines carrying ground water may be given an inner emulsion coating.			

According to the principles of AC impedance spectroscopy, when a protective film is formed on the metal surface, corrosion resistance increases,  $R_t$  values, impedance values and phase angle increase whereas  $C_{dl}$  values decrease (Figure 16).

It is inferred from Figures 4–14 and Table 2 that, when mild steel coated with emulsion coating is immersed in groundwater the corrosion resistance of mild steel is increased. This is due to the fact that the emulsion coating on the mild steel is stable in the presence of groundwater. The corrosion inhibition efficiency calculated from the charge transfer resistance values is found to be 98.11%. Inhibition efficiency calculated from the formula,  $IE = [(R_{t1} - R_{t2}) / R_{t1}] \cdot 100\%$ , where  $R_{t1}$  is the charge transfer resistance value in the presence of coating and  $R_{t2}$  is the charge transfer resistance value in the absence of coating.

### Implication

It is inferred from AC impedance spectral studies that the mild steel used in ground water storage tank may be given a coat of emulsion coating to improve the life time of the mild steel tank of ground water storage. Mild steel pipelines carrying ground water may be given an inner emulsion coating.

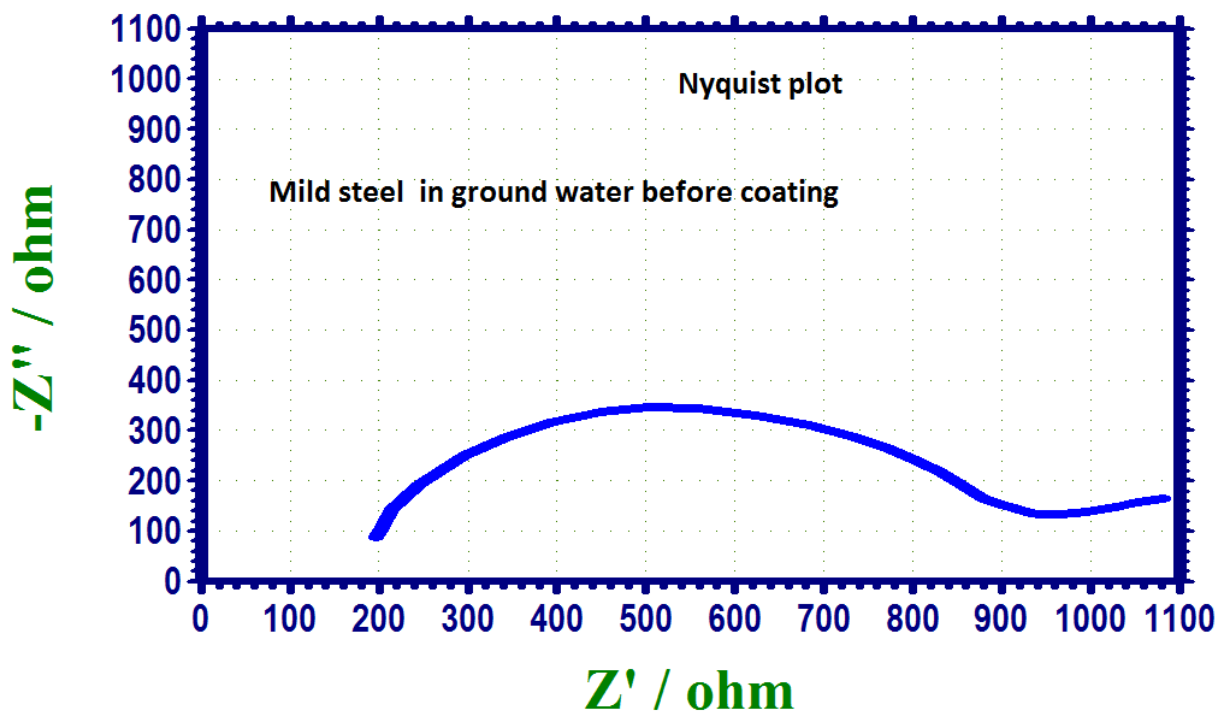


Figure 4. Nyquist plot of mild steel, before coating, immersed in ground water.

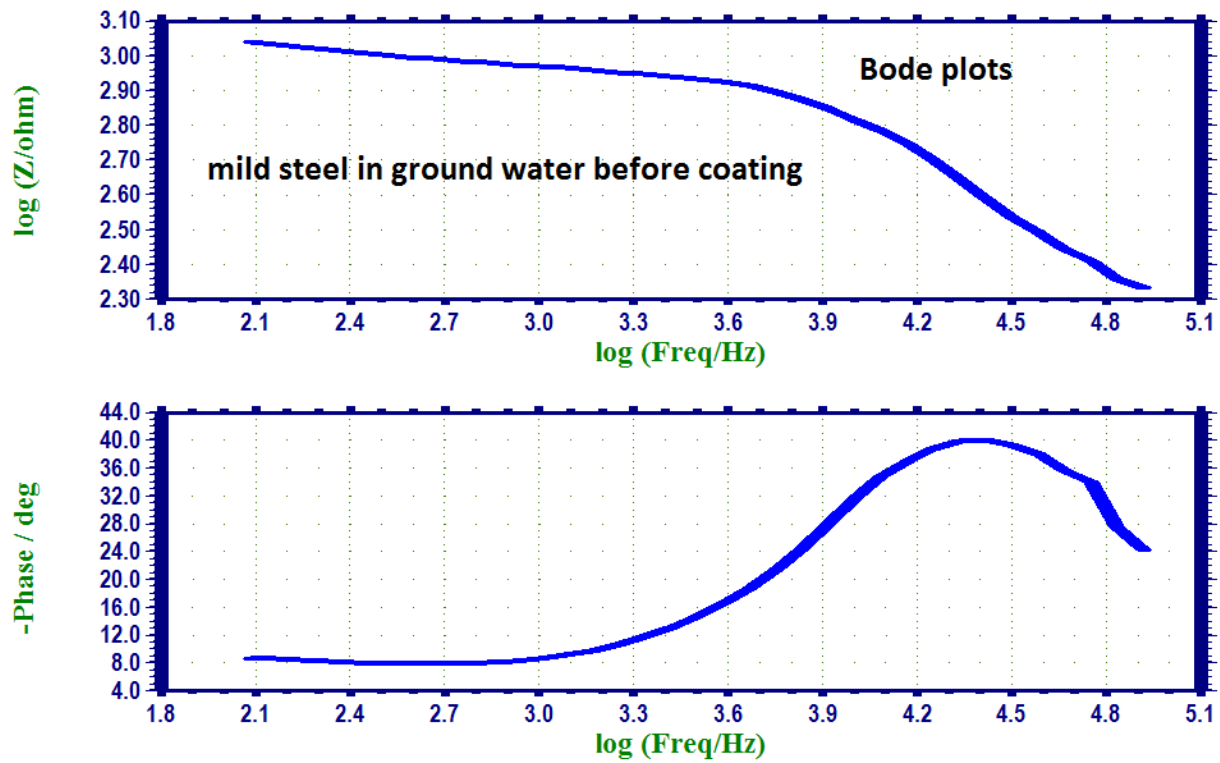


Figure 5. Bode plots of mild steel, before coating, immersed in ground water.

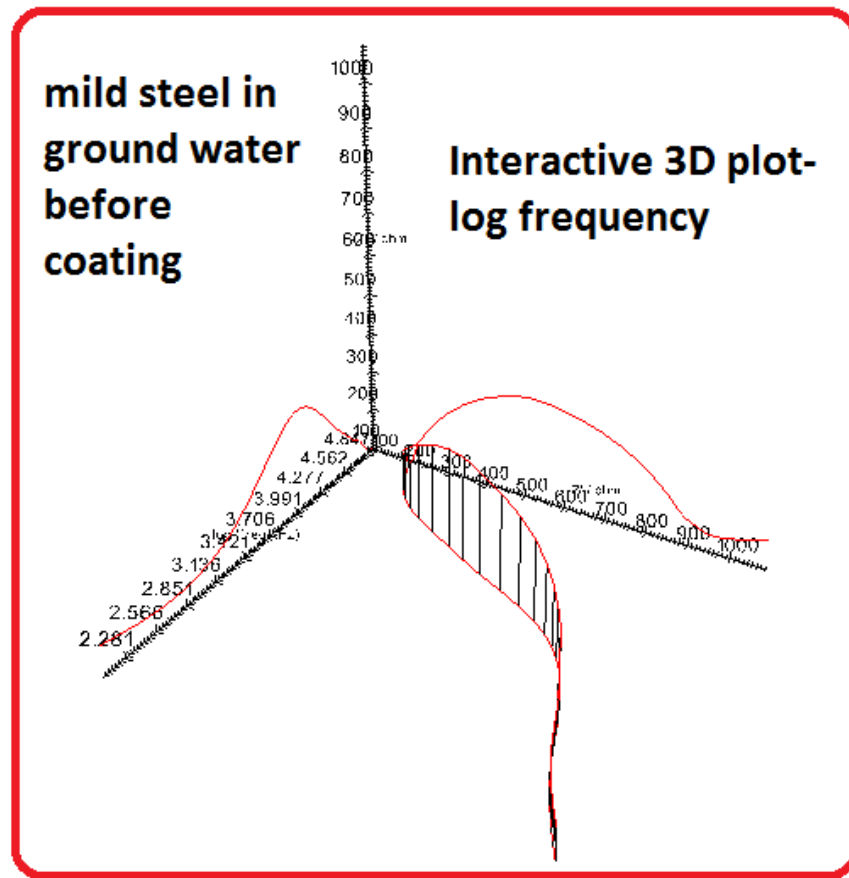


Figure 6. Interactive 3D plot of mild steel, before coating, immersed in ground water.

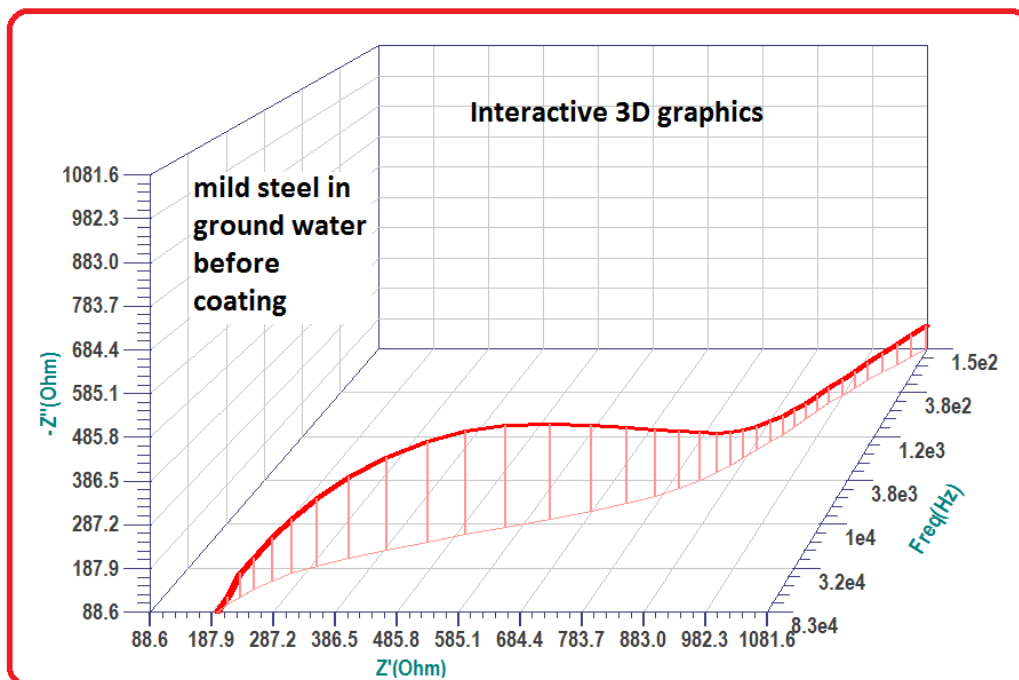


Figure 7. Interactive 3D graphics of mild steel, before coating, immersed in ground water.

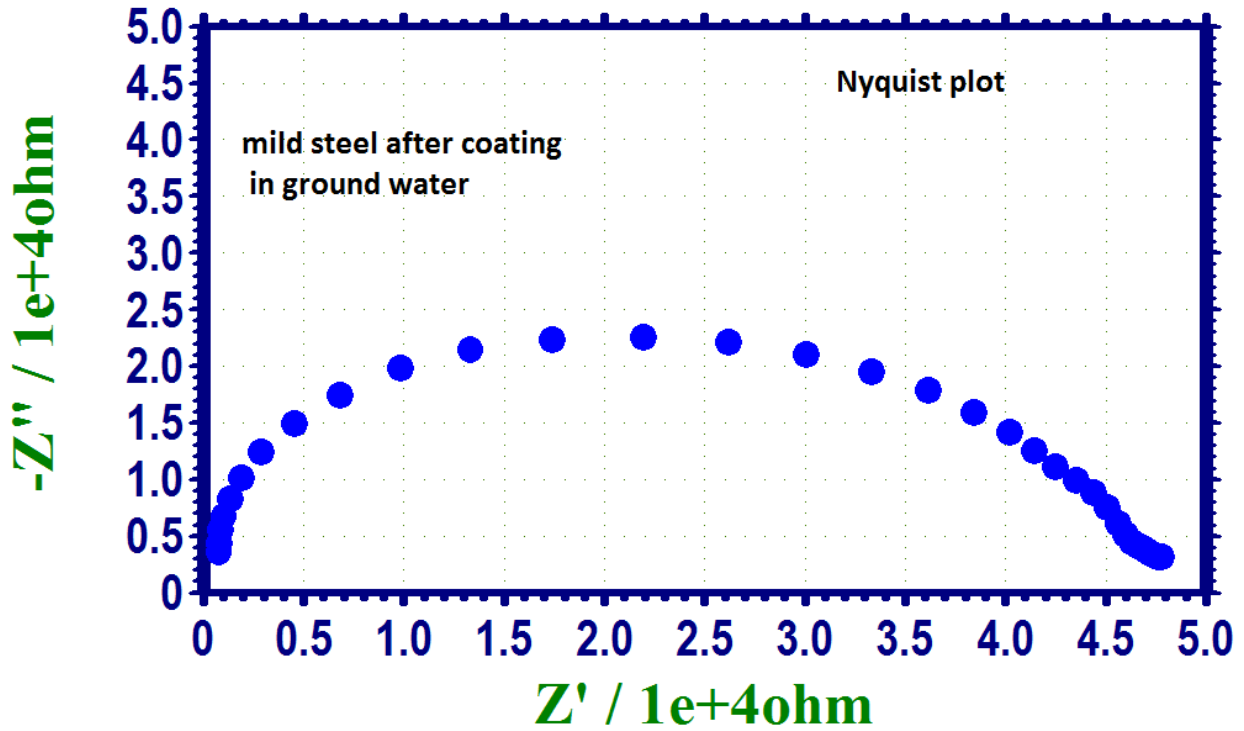


Figure 8. Nyquist plot of mild steel, after coating, immersed in ground water.

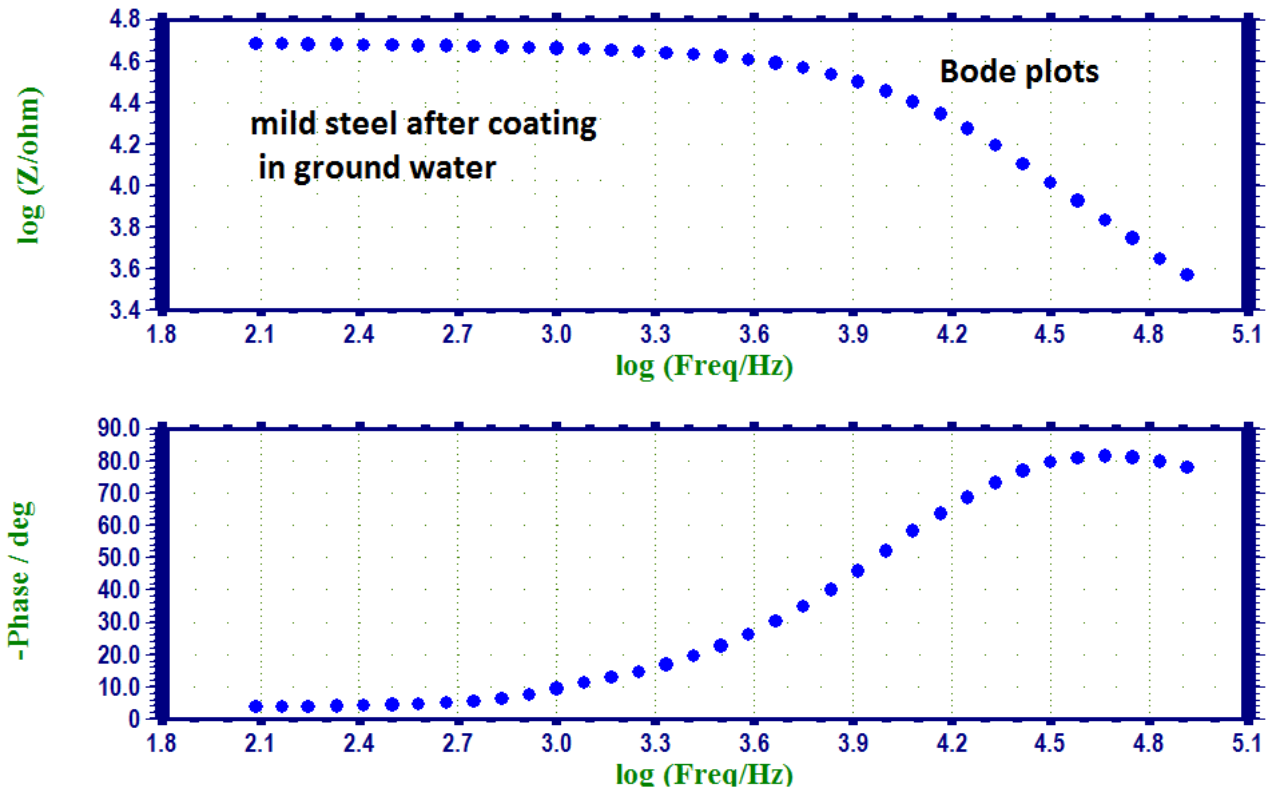


Figure 9. Bode plots of mild steel, after coating, immersed in ground water.

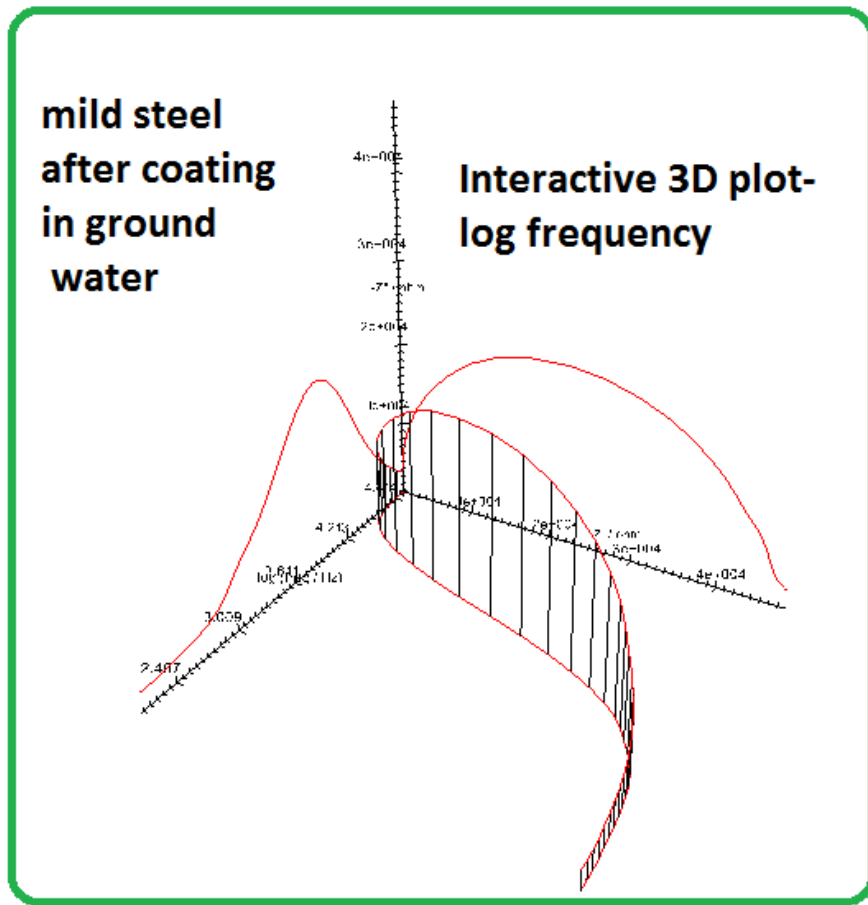


Figure 10. Interactive 3D plot of mild steel, after coating, immersed in ground water.

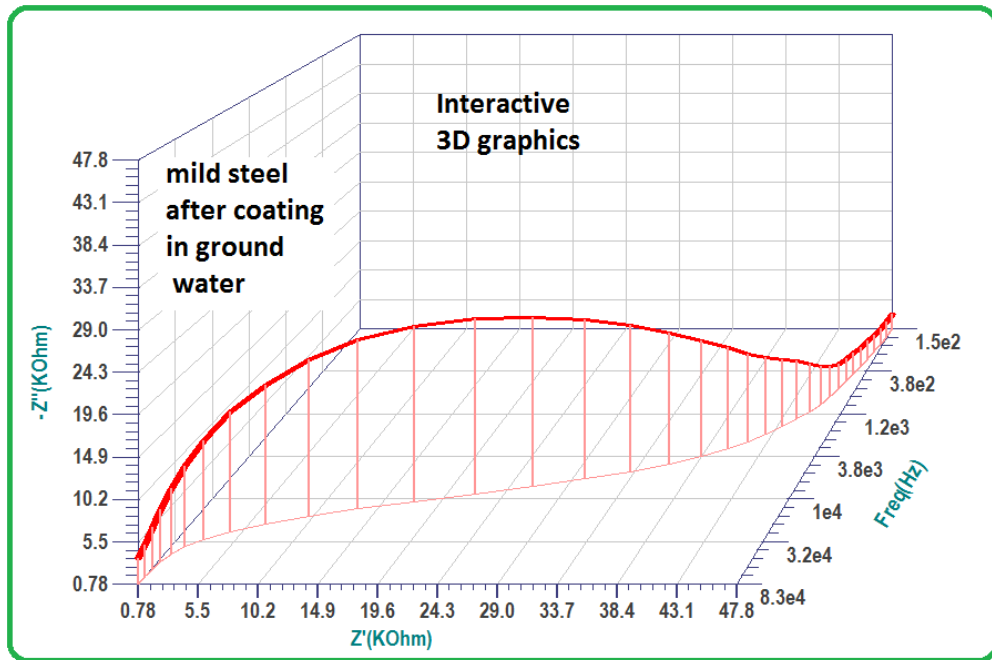


Figure 11. Interactive 3D graphics of mild steel, after coating, immersed in ground water.

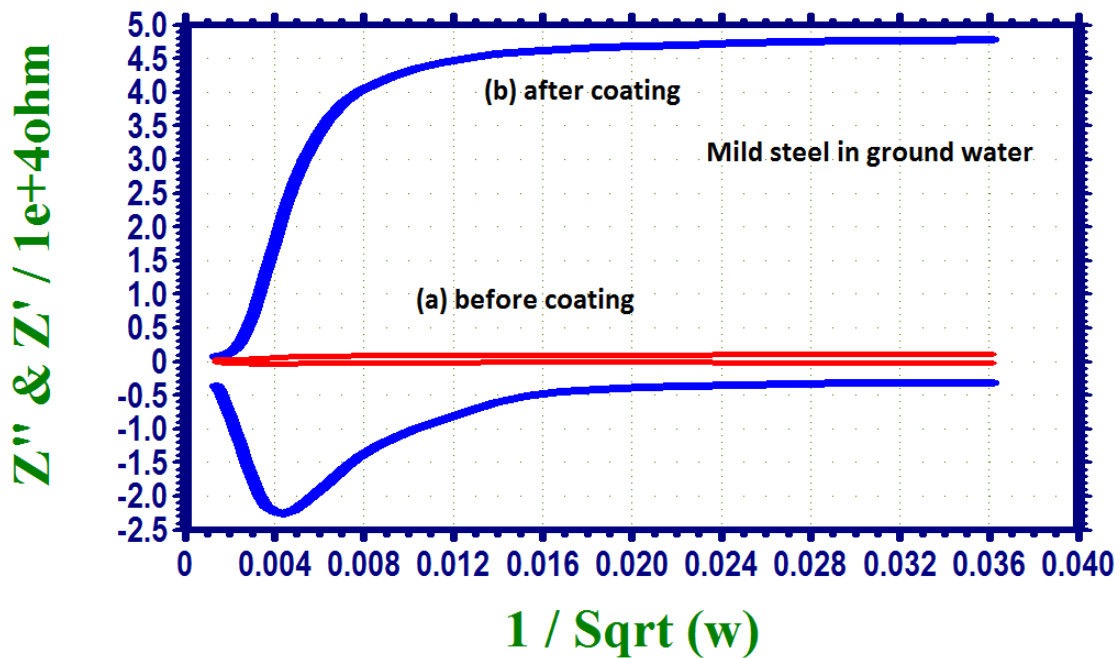


Figure 12. 1/Sq root of frequency vs.  $Z''$  and  $Z'$  plot.

It is observed from Figure 12 that for the blank system the plot is like a straight line. It runs parallel to the x-axis. The distance between  $Z''$  and  $Z'$  decreases.

For the inhibited system the distance between  $Z''$  and  $Z'$  increases. For a better inhibited system, the distance further increases.

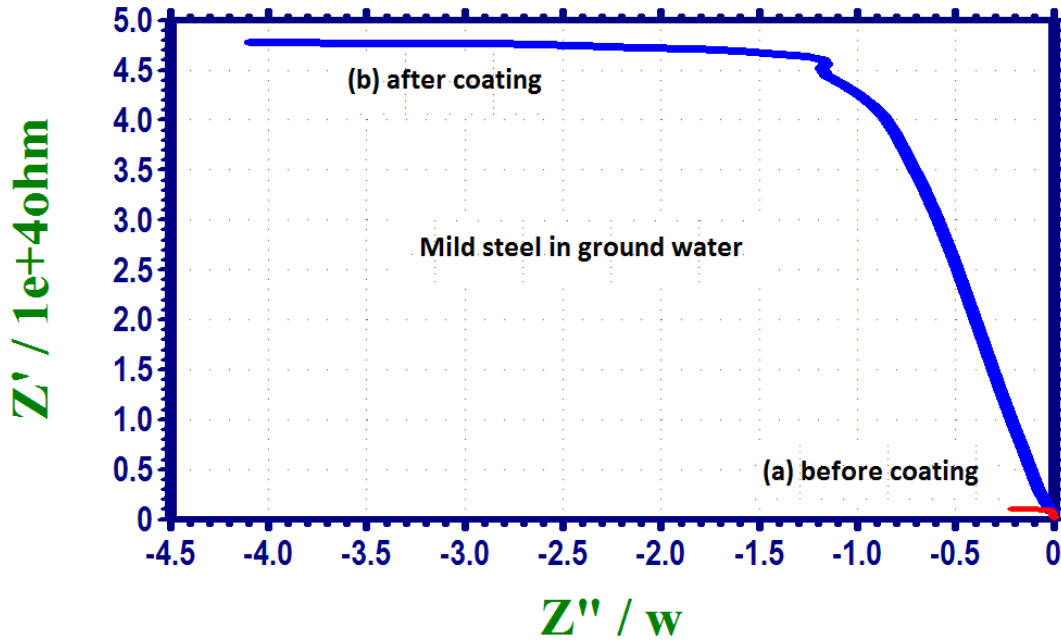


Figure 13.  $Z''/$  frequency vs.  $Z'$  plot.

It is observed from Figure 13, that for the uninhibited system the value of  $Z'$  is small. But for the inhibited system  $Z'$  value is very high.

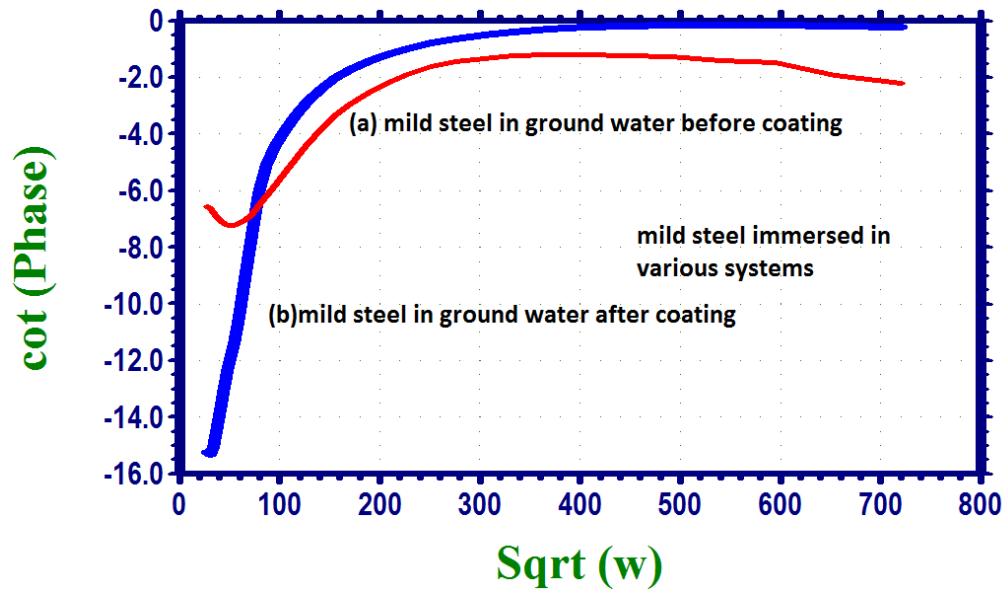
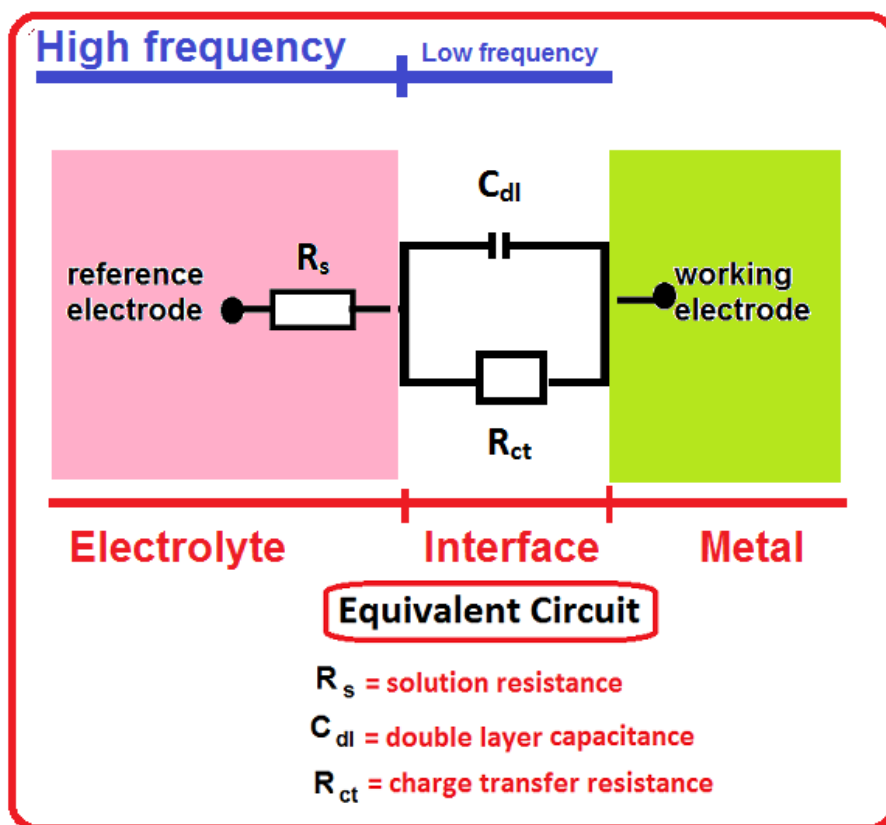
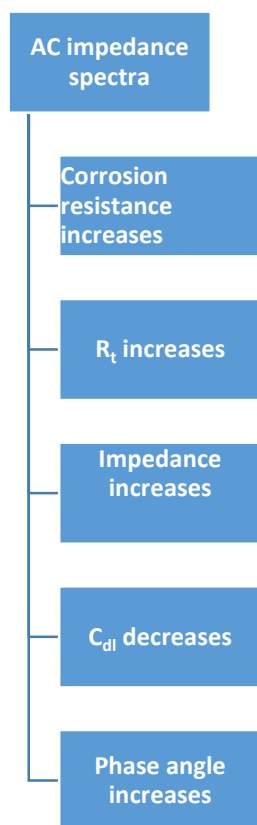


Figure 14. Square root of frequency vs.  $\cot$  angle plot.



**Figure 15.** Equivalent circuit for kinetic and diffusion processes.

It is observed from Figure 14 that when the square root of frequency increases the value of cot phase angle increases. For uninhibited system cot phase angle is more negative. For inhibited system this value is less negative. That is for inhibited system cot phase angle value is high. For uninhibited system this value is less.



**Figure 16.** Correlation among corrosion parameters of AC impedance spectroscopy.

#### *Analysis results of contact angle measurement*

Analysis of contact angle measurements are made to know the hydrophobic nature (water repelling nature) of metal surfaces [21–25]. If the contact angle is less than  $90^\circ$  it indicates that the surface is hydrophilic in nature. For hydrophobic surface the contact angle is greater than  $90^\circ$ . The images of the various surfaces are shown in Figures 17–19. It is inferred that the polished mild steel surface is hydrophobic in nature. The polished mild steel surface immersed in ground water becomes hydrophilic in nature. This is due to the formation of corrosion products such as iron oxide on the metal surface. The polished mild steel surface after coating becomes hydrophobic in nature. The surface becomes smoother and water repellent in nature. So, this surface offers corrosion inhibition efficiency greater than 90% as revealed by polarization study and AC impedance spectra.



**Figure 17.** Contact angle of polished mild steel surface.

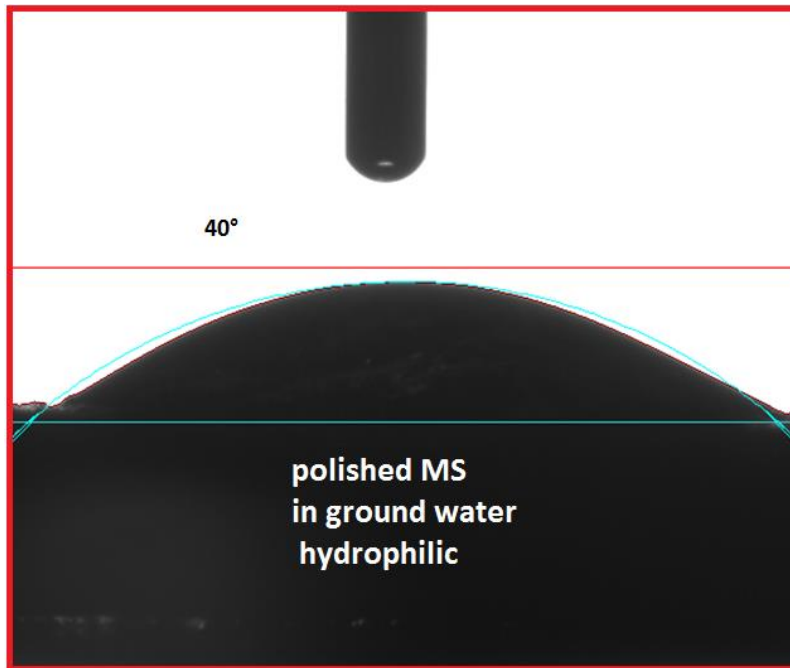


**Figure 18.** Contact angle of polished mild steel surface after immersion in ground water.

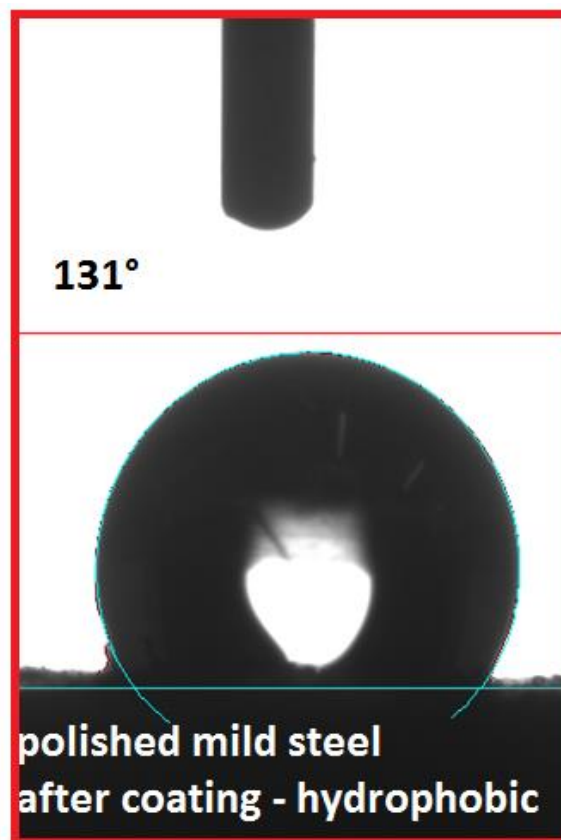


**Figure 19.** Contact angle of polished mild steel surface after coating.

### Analysis of SEM images

SEM images have been widely used in corrosion inhibition study [26–30]. For polished metal the surface is smooth. When the polished metal is placed in the corrosive medium (blank) the metal surface becomes rough. Pits are noticed. This is due to release of corrosion product and decay of metals. When a protective film is formed on the metal surface during corrosion inhibition process, the metal surface become smooth.

In the present study the SEM images of various surfaces are shown in Figure 20.

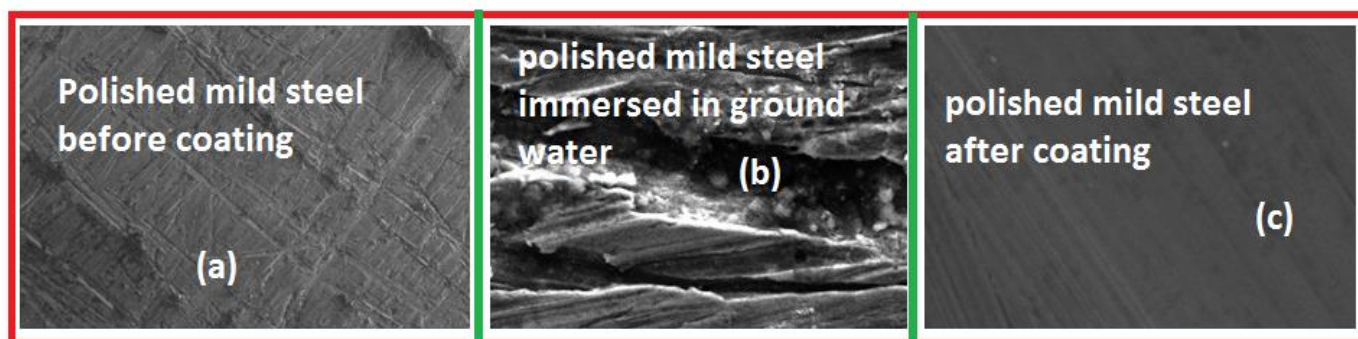


**Figure 20.** SEM images of various metal surfaces. (a) Polished mild steel before coating (b) polished mild steel immersed in ground water (c) polished mild steel after coating.

The SEM image of the polished mild steel before coating is shown in Figure 20a. The surface appears smooth. The slight roughness is due to the formation of iron oxides on the polished metal surface which undergoes mild corrosion in the atmosphere. When the metal surface is immersed in ground water pits are noticed on the metal surface (Figure 20b). The pits are due to the presence of aggressive ions present in the ground water. After emulsion coating the surface becomes smoother (Figure 20c).

### Analysis of AFM images and AFM parameters

In corrosion inhibition studies, AFM images and AFM parameters are used to investigate the nanofilms formed on metal surface during corrosion inhibition processes [31–35]. In the present study, the AFM images of polished mild steel (MS) before coating, MS immersed in ground water and Polished MS after emulsion coating were recorded and AFM parameters were derived from them. The AFM images are shown in Figures 21–23 and the AFM parameters are given in Table 3.

The average roughness for polished mild steel before coating is very small. When polished mild steel is immersed in ground water, this value becomes very high due to the formation of corrosion products. When polished mild steel is coated with emulsion coating, the surface is smoothed and hence the average roughness becomes lower than that of the corroded system but higher than that of the polished metal.

Similar observations are noted for RMS roughness ( $S_q$ ) and maximum peak-to-valley height ( $S_y$ ). The films are found to be in nano meter level.

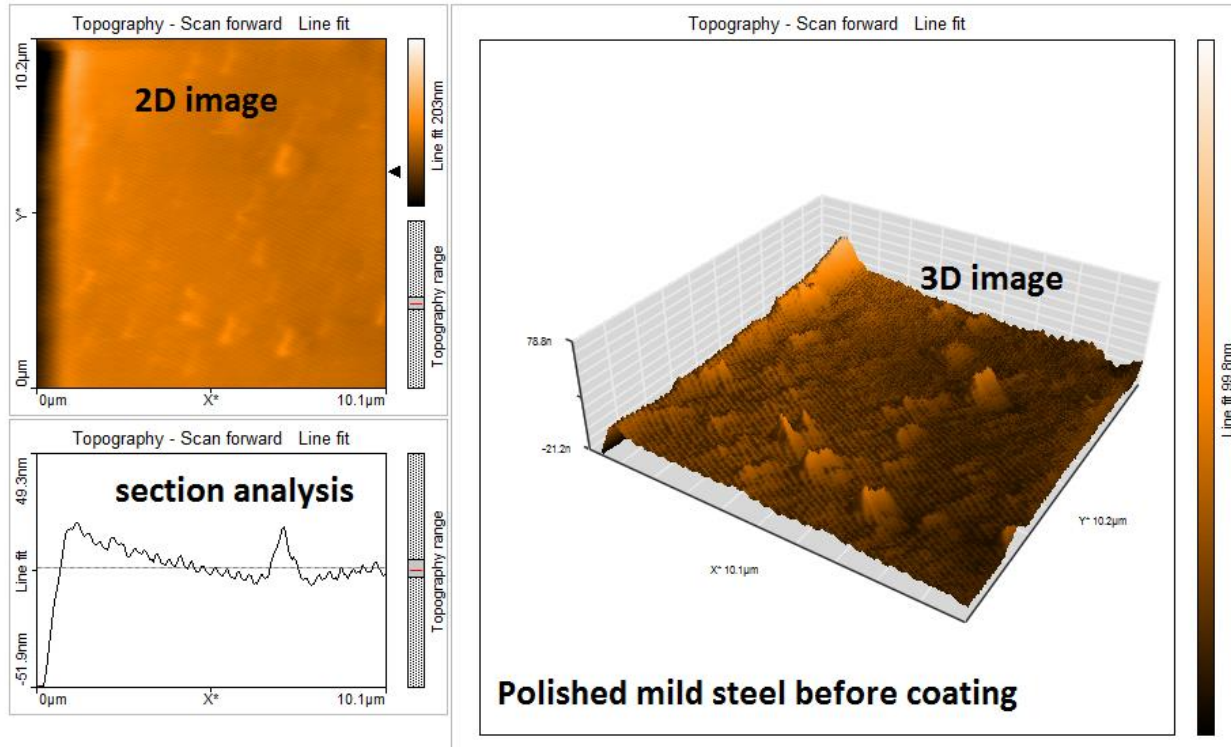


**Figure 21.** AFM images of polished mild steel before coating.

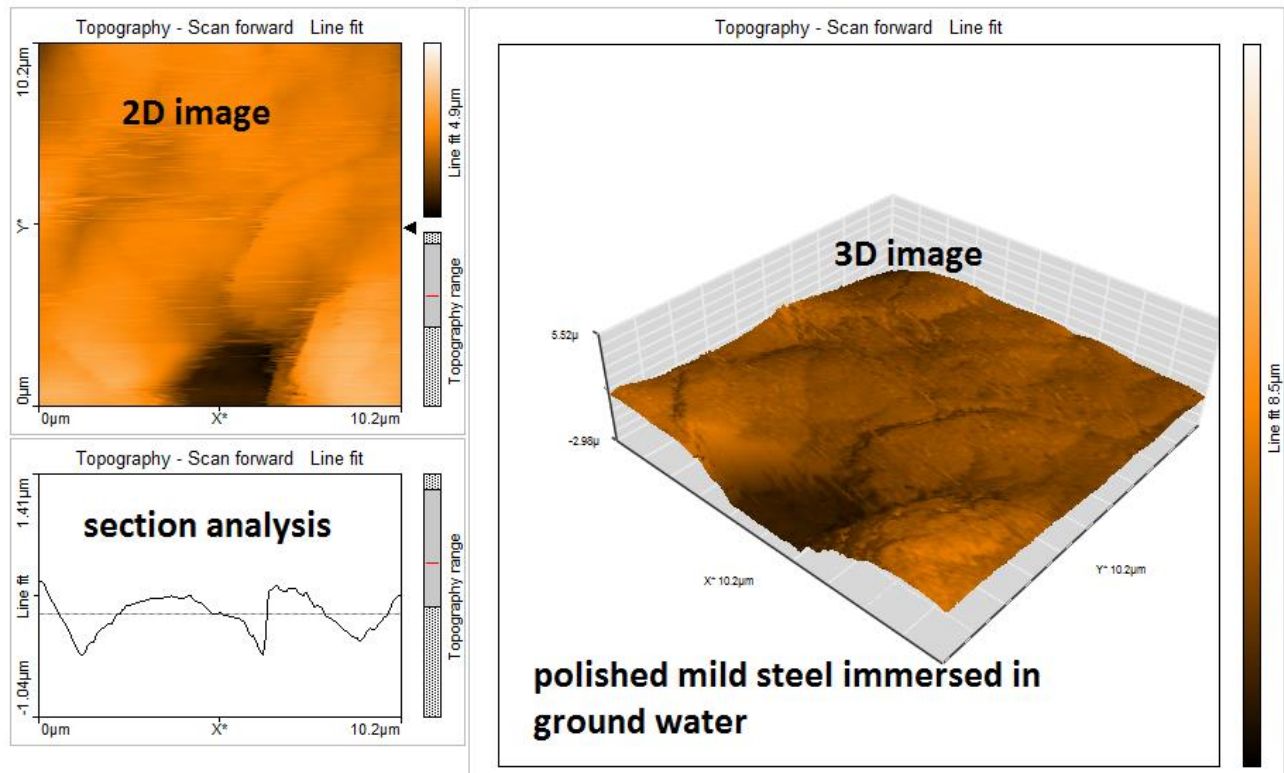


Figure 22. AFM images of polished mild steel after immersion in ground water.

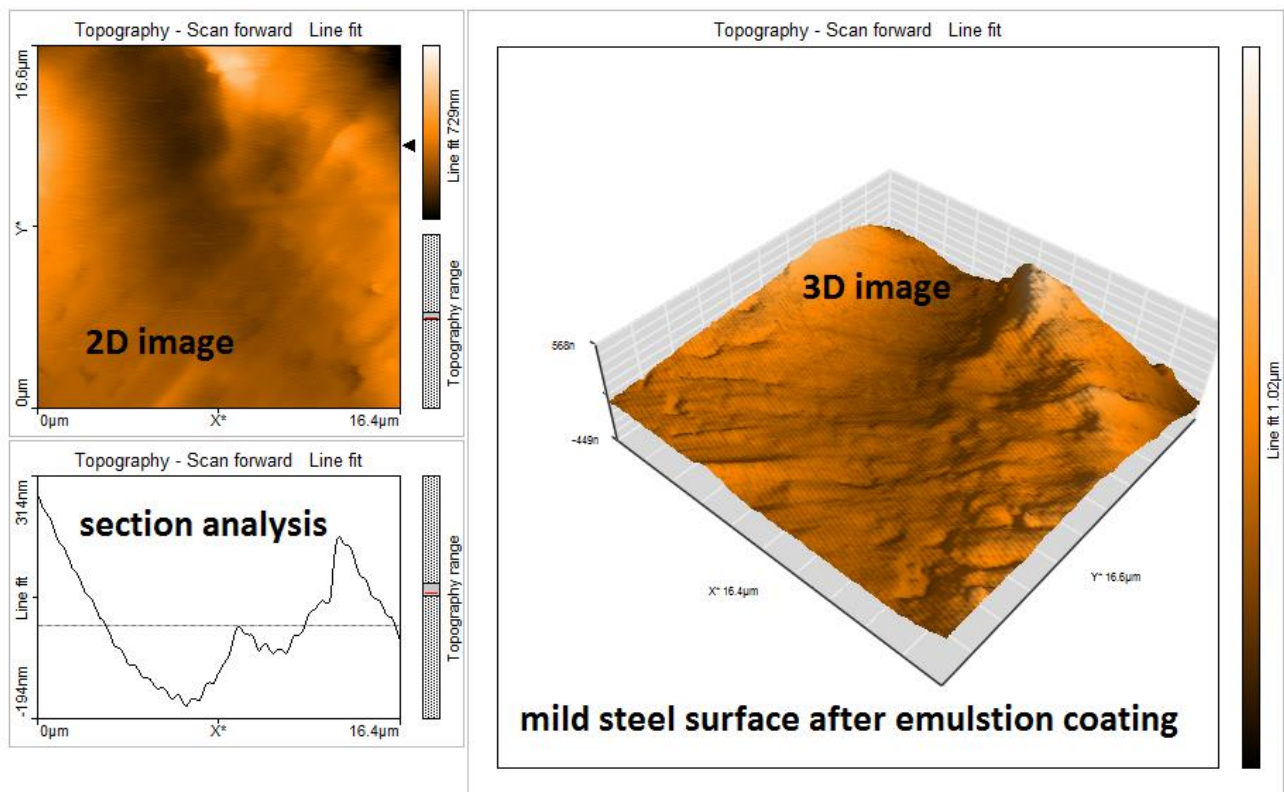


Figure 23. AFM images of polished mild steel after emulsion coating.

**Table 3.** AFM parameters (area roughness) of various mild steel surfaces.

Sample	RMS ( $S_q$ ) roughness (nm)	Average ( $S_a$ ) roughness (nm)	Maximum peak-to-valley height ( $S_y$ ) (nm)
Polished MS before coating	14.9 nm	8.3 nm	161.2 nm
MS immersed in ground water	540.1 nm	350.4 nm	3.5 $\mu\text{m}$
Polished MS after coating	84.0 nm	64.9 nm	639.1 nm

## Conclusion

- The corrosion resistance of mild steel immersed in groundwater before and after emulsion coating has been evaluated by electrochemical studies such as polarization study and AC impedance spectroscopy.
- When a protective film (emulsion coating) is formed on metal surface, corrosion resistance of the metal increases and hence LPR value increases and corrosion current decreases. Similarly, when a protective film is formed on the metal surface, corrosion resistance increases,  $R_t$  values, impedance values and phase angle increase whereas  $C_{dl}$  values decrease.
- Electrochemical studies reveal that the corrosion inhibition efficiency of mild steel after emulsion coating is found to be greater than 90%.
- Electrochemical studies lead to the conclusion that the mild steel tank used in water storing may be given a coat of emulsion coating to improve the life time of the mild steel tank.
- Mild steel pipelines carrying ground water may be given an inner emulsion coating.
- AFM study reveals that the film coating is at nano scale level.
- Contact angle measurement study reveals that after emulsion coating, the mild steel surface becomes hydrophobic in nature.
- It acquires water repelling nature
- So corrosion inhibition efficiency is greater than 95%.

## Scope for further study

The present work is undertaken to investigate the corrosion resistance of mild steel immersed in groundwater before and after coating with Weatherbond PRO (emulsion coating). The corrosion resistance has been evaluated by electrochemical studies such as polarization study and AC impedance spectra.

In future the following study can be under taken

- Instead of mild steel, aluminium, copper or zinc can be used.
- Instead of groundwater, simulated oil well water or sea water can be used.
- Surface analysis such as EDAX, FTIR, *etc.* can be used.

## References

1. K. Yang, X. Wang, I. Lynch, Z. Guo, P. Zhang and L. Wu, Green construction of MBI corrosion-resistant interfaces modified NZVI@MOFs-regulated 3D PAN cryogel film to enhance Cr(VI) removal, *Sep. Purif. Technol.*, 2024, **333**, 125902. doi: [10.1016/j.seppur.2023.125902](https://doi.org/10.1016/j.seppur.2023.125902)
2. X.P. Hu, Y.H. Zhang, C.B. Liu and H.Z. Cui, Polydopamine wrapped polyaniline nanosheets: Synthesis and anticorrosion application for waterborne epoxy coatings, *J. Mater. Sci. Technol.*, 2024, **176**, 155–166. doi: [10.1016/j.jmst.2023.07.054](https://doi.org/10.1016/j.jmst.2023.07.054)
3. N. Ghamari, R. Ahmadi, M.S. Sheikhzadeh and A. Afshar, Development of PDMS/TiO<sub>2</sub>/Ag<sub>3</sub>PO<sub>4</sub> antibacterial coating on 316L/PDMS implants: Evaluation of superhydrophobicity, bio-corrosion, mechanical behaviour, surface nanostructure and chemistry, *J. Mech. Behav. Biomed. Mater.*, 2024, **150**, 106315. doi: [10.1016/j.jmbbm.2023.106315](https://doi.org/10.1016/j.jmbbm.2023.106315)
4. N. Chen, J. He, H. Xuan, J. Jin, K. Yu, M. Shi and C. Yan, Dual-functional Polyindole/MXene composite for superior proton storage and corrosion protection, *Composites, Part B*, 2024, **270**, 111145. doi: [10.1016/j.compositesb.2023.111145](https://doi.org/10.1016/j.compositesb.2023.111145)
5. Y. Zhang, H. Li, L. Cui, W. Yang, G. Ma, R. Chen, P. Guo, P. Ke and A. Wang, Comparative study on tribocorrosion behavior of hydrogenated/hydrogen-free amorphous carbon coated WC-based cermet in 3.5 wt.% NaCl solution, *Corros. Sci.*, 2024, **227**, 111738. doi: [10.1016/j.corsci.2023.111738](https://doi.org/10.1016/j.corsci.2023.111738)
6. K. Wei, Y. Wei, Y. Zhang, V. Kasneryk, M. Serdechnova, H. Wang, Z. Zhang, Y. Yuan, C. Blawert, M.L. Zheludkevich and F. Chen, *In Situ* synthesis of ZIF-8 loaded with 8-hydroxyquinoline composite via a host-guest nanoconfinement strategy for high-performance corrosion protection, *Corros. Sci.*, 2024, **227**, 111731. doi: [10.1016/j.corsci.2023.111731](https://doi.org/10.1016/j.corsci.2023.111731)
7. Y. Xia, L. Tong, X. Feng, H. Xiang, Y. He and X. Liu, Effects of polydopamine functionalized graphitic carbon nitride cerium oxide nanofiller on the corrosion resistance of epoxy coating, *Prog. Org. Coat.*, 2024, **187**, 108111. doi: [10.1016/j.porgcoat.2023.108111](https://doi.org/10.1016/j.porgcoat.2023.108111)
8. A.S. Vijayan, A. Joseph, A. Joseph, T.S. Abhijith, B.G. Nair and V. Sajith, Polydopamine functionalised ceria-zirconia nanoparticles embedded water-borne epoxy nanocomposite for anti-biofouling coatings, *Prog. Org. Coat.*, 2024, **187**, 108094. doi: [10.1016/j.porgcoat.2023.108094](https://doi.org/10.1016/j.porgcoat.2023.108094)
9. H. Wan, Z.L. Cheng, D. Song and C. Chen, Preparation and performance study of waterborne epoxy resin/non-covalent modified graphene oxide hydrogen barrier coatings, *Int. J. Hydrogen Energy*, 2024, **53**, 218–228. doi: [10.1016/j.ijhydene.2023.12.051](https://doi.org/10.1016/j.ijhydene.2023.12.051)

10. C. Li, Y. Liu, Q. Yu, S. Sun, S. Liu, C. Zhao, X. Wang, S. Yang, B. Yu, M. Cai, F. Zhou and W. Liu, A composite coating based on  $Ti_3C_2T_x$  MXene and M16 corrosion inhibitor for self-healing anti-corrosion and wear resistance, *Surf. Coat. Technol.*, 2024, **476**, 130281. doi: [10.1016/j.surfcoat.2023.130281](https://doi.org/10.1016/j.surfcoat.2023.130281)
11. R.L. Minagalavar, M.R. Rathod, S.K. Rajappa and A.M. Sajjan, Experimental and Theoretical Investigations of *Cordia Obliqua* Leaves Extract as an Environmentally Benign Inhibitor for Mild Steel Corrosion in a 1 M HCl Solution, *Port. Electrochim. Acta*, 2024, **42**, no. 4, 233–254. doi: [10.4152/pea.2024420401](https://doi.org/10.4152/pea.2024420401)
12. Z.A. El Caid, D.B. Left and M. Zertoubi, An exploratory assessment supported by experimental and modeling approaches for dinitrophenylhydrazine compound as a potent corrosion inhibitor for carbon steel in sulfuric acid solution, *J. Mol. Struct.*, 2024, **1300**, 137218. doi: [10.1016/j.molstruc.2023.137218](https://doi.org/10.1016/j.molstruc.2023.137218)
13. R. Khanna, V. Kalia, R. Kumar, R. Kumar, P. Kumar, H. Dahiya, P. Pahuja, G. Jhaa and H. Kumar, Synergistic experimental and computational approaches for evaluating pyrazole Schiff bases as corrosion inhibitor for mild steel in acidic medium, *J. Mol. Struct.*, 2024, **1297**, 136845. doi: [10.1016/j.molstruc.2023.136845](https://doi.org/10.1016/j.molstruc.2023.136845)
14. P.H. Rao, S. Rao, P. Shree S.S. Prashanth and G.K. Renuka, Corrosion mitigation of mild steel in 1 M HCl acid using an expired drug: An experimental approach, *Inorg. Chem. Commun.*, 2024, **160**, 111871. doi: [10.1016/j.inoche.2023.111871](https://doi.org/10.1016/j.inoche.2023.111871)
15. K. Li, H. Zheng, J.-X. Lu, W. Li and C.S. Poon, Role of encapsulated corrosion inhibitor on the anti-corrosion performance of reinforcing steel in lightweight concrete, *Cem. Concr. Compos.*, 2024, **146**, no. 5, 105388. doi: [10.1016/j.cemconcomp.2023.105388](https://doi.org/10.1016/j.cemconcomp.2023.105388)
16. A. Chraka, I. Raissouni, J. Kassout, M. Ezzaki, N.B. Seddik, F. Janoub, M. Manssouri, H. Belcadi, A. Ibn Mansour and D. Bouchta, Understanding the synergistic inhibition effect of hydrosol extract derivatives as eco-friendly anti-corrosive for copper alloy: GC–MS Identification, An Electrochemical, surface morphology and computational modeling, *J. Mol. Liq.*, 2023, **392**, 123507. doi: [10.1016/j.molliq.2023.123507](https://doi.org/10.1016/j.molliq.2023.123507)
17. R. Sudhakaran, T. Deepa, M. Thirumavalavan, S.Q. Sabarimuthu, S. Babu, T. Asokan, P.B. Raja, N. Arumugam, K. Perumal, S. Djearamane, L.-H. Tey and S. Kayarohanam, Trisodium citrate as a potential and eco-friendly corrosion inhibitor of copper in potable water, *J. King Saud Univ., Sci.*, 2023, **35**, no. 8, 102907. doi: [10.1016/j.jksus.2023.102907](https://doi.org/10.1016/j.jksus.2023.102907)
18. P. Vashishth, H. Bairagi, R. Narang, S.K. Shukla, L.O. Olasunkanmi, E.E. Ebenso and B. Mangla, Experimental investigation of sustainable Corrosion Inhibitor Albumin on low-carbon steel in 1N HCl and 1N  $H_2SO_4$ , *Res. Surf. Interfaces*, 2023, **13**, 100155. doi: [10.1016/j.rsurfi.2023.100155](https://doi.org/10.1016/j.rsurfi.2023.100155)
19. R. Jalab, M. Saad, A. Benali, I.A. Hussein and M. Khaled, Biodegradable polysaccharide grafted polyacrylamide inhibitor for corrosion in  $CO_2$ - saturated saline solution, *Heliyon*, 2023, **9**, no. 10, e20304. doi: [10.1016/j.heliyon.2023.e20304](https://doi.org/10.1016/j.heliyon.2023.e20304)

- 
20. H. Bairagi, P. Vashishth, R. Narang, S.K. Shukla and B. Mangla, Experimental and Computational Studies of a Novel Metal Oxide Nanoparticle/Conducting Polymer Nanocomposite (TiO<sub>2</sub>/PVP) as a Corrosion Inhibitor on Low-Carbon Steel in Diprotic Acidic Medium, *Ind. Eng. Chem. Res.*, 2023, **62**, no. 28, 10982–11000. doi: [10.1021/acs.iecr.3c00099](https://doi.org/10.1021/acs.iecr.3c00099)
  21. N. Timoudan, A. Titi, M. El Faydy, F. Benhiba, R. Touzani, I. Warad, A. Bellaouchou, Ali Alsulmi, B. Dikici, F. Bentiss and A. Zarrouk, Investigation of the mechanisms and adsorption of a new pyrazole derivative against corrosion of carbon steel in hydrochloric acid solution: Experimental methods and theoretical calculations, *Colloids Surf., A*, 2024, **682**, 132771. doi: [10.1016/j.colsurfa.2023.132771](https://doi.org/10.1016/j.colsurfa.2023.132771)
  22. R. Khanna, V. Kalia, R. Kumar, P. Kumar, H. Dahiya, P. Pahuja, G. Jhaa and H. Kumar, Synergistic experimental and computational approaches for evaluating pyrazole Schiff bases as corrosion inhibitor for mild steel in acidic medium, *J. Mol. Struct.*, 2024, **1297**, 136845. doi: [10.1016/j.molstruc.2023.136845](https://doi.org/10.1016/j.molstruc.2023.136845)
  23. A. Elsamman, K.F. Khaled, S.A. Halim and N.S. Abdelshafi, A critical view of the QSAR model for the prediction of a new bispyrazole derivative BPYR-P as a corrosion inhibitor for 304 SS in a 1.0 M HCl solution, *J. Mol. Struct.*, 2024, **1297**, 136728. doi: [10.1016/j.molstruc.2023.136728](https://doi.org/10.1016/j.molstruc.2023.136728)
  24. P.H. Renuka, S. Rao, P. Rao, S.S. Shree and G.K. Prashanth, Corrosion mitigation of mild steel in 1 M HCl acid using an expired drug: An experimental approach, *Inorg. Chem. Commun.*, 2024, **160**, 111871. doi: [10.1016/j.inoche.2023.111871](https://doi.org/10.1016/j.inoche.2023.111871)
  25. J. He, X. Li, B. Xie, Y. He, C. Lai, B. Dou, J Feng, M. Liu, R. Ji and W. Zhao, Exploration of rigid double schiff base with a symmetrical plane as highly effective corrosion inhibitor for mild steel in hydrochloric acid environment: Experimental and theoretical approaches, *Mater. Chem. Phys.*, 2024, **313**, 128785. doi: [10.1016/j.matchemphys.2023.128785](https://doi.org/10.1016/j.matchemphys.2023.128785)
  26. H. Assad, S.K. Saha, N. Kang, S. Kumar, P.K. Sharma, H. Dahiya, A. Thakur, S. Sharma, R. Ganjoo and A. Kumar, Electrochemical and computational insights into the utilization of 2,2-dithio bisbenzothiazole as a sustainable corrosion inhibitor for mild steel in low pH medium, *Environ. Res.*, 2024, **242**, 117640. doi: [10.1016/j.envres.2023.117640](https://doi.org/10.1016/j.envres.2023.117640)
  27. G.A. Gaber, M.M. Soliman, Z.A. Nasr and A.M. Hyba, Comprehensive investigation of sustainable corrosion inhibitors on Cu–Zn alloy in simulated cooling water: Electrochemical explorations, SEM/EDX analysis, and DFT/molecular simulations utilizing expired Bepotastine-B as a green inhibitor, *Sustainable Chem. Pharm.*, 2024, **37**, 101340. doi: [10.1016/j.scp.2023.101340](https://doi.org/10.1016/j.scp.2023.101340)
  28. A.E.-A.S. Fouda, S.E.H. Etaiw, D.M. Abd El-Aziz, A.A. El-Hossiany and U.A. Elbaz, Experimental and theoretical studies of the efficiency of metal–organic frameworks (MOFs) in preventing aluminum corrosion in hydrochloric acid solution, *BMC Chem.*, 2024, **18**, no.1, 21. doi: [10.1186/s13065-024-01121-6](https://doi.org/10.1186/s13065-024-01121-6)

- 
29. H. Bao, Y. Lian, Z. Qiao, S. Zhang, X. Meng, K. Ma, D. Zhu, J. Zhao and H. Zhang, N-doped carbon quantum dots as corrosion inhibitor for ultra-high voltage etched Al foil, *Surf. Coat. Technol.*, 2024, **476**, 130240. doi: [10.1016/j.surfcoat.2023.130240](https://doi.org/10.1016/j.surfcoat.2023.130240)
  30. W. Ettahiri, M. Adardour, E. Ech-chihbi, M. Azam, R. Salim, S. Dalbouha, K. Min, Z. Rais, A. Baouid and M. Taleb, 1,2,3-triazolyl-linked benzimidazolone derivatives as new eco-friendly corrosion inhibitors for mild steel in 1 M HCl solution: Experimental and computational studies, *Colloids Surf., A*, 2024, **681**, 132727. doi: [10.1016/j.colsurfa.2023.132727](https://doi.org/10.1016/j.colsurfa.2023.132727)
  31. K. Dahmani, M. Galai, M. Rbaa, A. Ech-Chebab, N. Errahmany, L. Guo, A.A. AlObaid, A. Hmada, I. Warad, B. lakhrissi, M. Ebn Touhami and M. Cherkaoui, Evaluating the efficacy of synthesized quinoline derivatives as Corrosion inhibitors for mild steel in acidic environments: An analysis using electrochemical, computational, and surface techniques, *J. Mol. Struct.*, 2024, **1295**, 136514. doi: [10.1016/j.molstruc.2023.136514](https://doi.org/10.1016/j.molstruc.2023.136514)
  32. K. Haruna and T.A. Saleh, Dopamine functionalized graphene oxide (DGO) as a corrosion inhibitor against X60 carbon steel corrosion in a simulated acidizing environment; An electrochemical, weight loss, SERS, and computational study, *Surf. Interfaces*, 2024, **44**, 103688. doi: [10.1016/j.surfin.2023.103688](https://doi.org/10.1016/j.surfin.2023.103688)
  33. Sheetal, A.K. Singh, M. Singh, S. Thakur, B. Pani, J. Singh, S. Zamindar and P. Banerjee, Understanding of remarkable corrosion combating action of N-(benzo[d]thiazol-2-yl)-1-(2-substituted phenyl) methanimines: Electrochemical, surface and computational approach, *Inorg. Chem. Commun.*, 2024, **159**, 111736. doi: [10.1016/j.inoche.2023.111736](https://doi.org/10.1016/j.inoche.2023.111736)
  34. Y. Liu, X. Guan and J. Shi, Synergistic inhibition of molybdate and phytate on chloride-induced corrosion of carbon steel in simulated concrete pore solutions, *Cem. Concr. Compos.*, 2024, **145**, 105366. doi: [10.1016/j.cemconcomp.2023.105366](https://doi.org/10.1016/j.cemconcomp.2023.105366)
  35. M. Galai, K. Dahmani, O. Kharbouch, M. Rbaa, N. Alzeqri, L. Guo, A.A. AlObaid, A. Hmada, N. Dkhireche, E. Ech-chihbi, M. Ouakki, M.E. Touhami and I. Warad, Surface analysis and interface properties of a newly synthesized quinoline-derivative corrosion inhibitor for mild steel in acid pickling bath: Mechanistic exploration through electrochemical, XPS, AFM, contact angle, SEM/EDS and computational studies, *J. Phys. Chem. Solids*, 2024, **184**, 111681. doi: [10.1016/j.jpcs.2023.111681](https://doi.org/10.1016/j.jpcs.2023.111681)

